Asymmetric Polyurethane Membrane with *In Situ*-Generated Nano-TiO_2 as Wound Dressing

Yi Chen,[1] Lidan Yan,[2] Tun Yuan,[3] Qiyi Zhang,[2] Haojun Fan[1]

[1]*National Engineering Laboratory for Clean Technology of Leather Manufacture, Sichuan University, Chengdu 610065, People's Republic of China*
[2]*School of Chemical Engineering, Sichuan University, Chengdu 610065, People's Republic of China*
[3]*Engineering Research Center in Biomaterials, Sichuan University, Chengdu 610065, People's Republic of China*

Received 9 October 2009; accepted 13 May 2010
DOI 10.1002/app.32813
Published online 19 August 2010 in Wiley Online Library (wileyonlinelibrary.com).

ABSTRACT: For potential application as an ideal wound dressing, a novel asymmetric polyurethane membrane with *in situ*-generated nano-TiO_2 (PUNT) was successfully prepared via a combination of solvent evaporation, wet phase inversion, and organic–inorganic hybridization. According to this combination method, the PUNT membrane consisted of an integral and dense skin layer supported by a porous sublayer, with nano-TiO_2 particles dispersed evenly throughout the sample. The skin layer was found to be impermeable to bacteria penetration, and the porous sublayer was designed for absorbing high amounts of exudates. Nitrogen adsorption/desorption experiment proved that extra mesopores were created in the PUNT membrane after organic–inorganic hybridization, which resulted in promoted gas permeability, water vapor transmission rate, and exudate absorption capability. The PUNT membrane, as a consequence, could accelerate gas exchange and also provide an optimal level of moisture over the wound beds without risking dehydration or exudate accumulation. Shake flask testing and cell culture (L929) assay indicated that the PUNT membrane exhibited antibacterial activity against *Pseudomonas aeruginosa*, *Escherichia coli*, and *Staphylococcus aureus*, whereas showed no cytotoxicity. From *in vivo* animal studies, the curative effect of PUNT membrane was found to be better than gauze and a commercial polyurethane membrane dressing. These results indicated that the PUNT membrane with multifunctions prepared in this study has potential for application as an ideal wound dressing. © 2010 Wiley Periodicals, Inc. J Appl Polym Sci 119: 1532–1541, 2011

Key words: polyurethanes; nanocomposites; films; biomaterials

INTRODUCTION

In the treatment of burns, donor site wounds, skin ulcers, and surgical wounds, immediate coverage of wound beds with dressings is necessary for rapid and proper healing. According to modern medical insights,[1,2] there are several functions that are desirable for an ideal wound dressing: (1) a suitable water vapor transmission rate (WVTR) that produces a moist environment on the wound beds, without risking dehydration or exudate accumulation; (2) sufficient gas permeability for oxygen-requiring reparative processes; (3) a high level of fluid absorption capability to remove excessive exudates that contain nutrients for bacteria from the wound beds; (4) a good barrier against the penetration of infection-causing microorganisms; (5) antibacterial activity to suppress bacteria growth beneath the dressing; and (6) the absence of any cytotoxic effects in case of secondary damage to the neonatal tissues.

Among various synthetic dressings in the market, polyurethane (PU) membrane dressings are increasingly popular considering their good physical strength, abrasion resistance, fatigue life, and tissue compatibility.[3] However, their totally dense structure results in certain inconvenient limitations, including low water vapor/gas transmission rate and poor fluid absorption capability. These disadvantages frequently cause exudate accumulation and infection-related complications in clinic cases. Meanwhile, low gas permeability inhibits oxygen exchange through the dressings, which is detrimental to cell migration and mitosis. Another major problem with PU membrane dressings is the incorporation of aggressive antimicrobial compounds. Despite their efficiency against bacteria contamination, these compounds may exhibit cytotoxic effects to newly formed tissue. Thus, it seems that the PU membrane dressings currently available are far from ideal, and modification is necessary to overcome the above limitations.

Nowadays, asymmetric polymer membranes have found numerous application fields, ranging from gas

Correspondence to: H. Fan (fanhaojun@scu.edu.cn).
Contract grant sponsor: Hi-tech Research and Development Program of China (863 Program); contract grant number: 2007AA03Z341.

separation, textile to biomedical industries.[4,5] Among the methods proposed to prepare asymmetric membranes, wet phase inversion method is the most widely used technique. In this method, a casting polymer solution containing solvent is immersed into a nonsolvent coagulant that has a low mutual affinity to the solvent. Because of delayed phase separation at the outmost interface region of the casting solution, a compact top layer with porous substructure can be obtained. If this asymmetric membrane is used as a wound dressing, there seems to be two disadvantages. First, the top layer formed by this method is quite thin (less than 1 μm),[5–7] which cannot prevent excessive water vapor evaporation from the wound beds. Second, although the top layer has a compact structure, it contains defects[5–8] that significantly compromise its barrier function against outside contamination.

Polymeric nanocomposites have been established as an exciting new class of materials that are particle-filled, with at least one dimension of the dispersed particles being in the nanometer range, which usually exhibit superior performances compared with conventional filler composites. Basically, the most commonly used methods to prepare polymeric nanocomposites thus far are melt mixing and solution blending.[9] As preformed nanoparticles are chemically fused together, it is hard for these two methods to achieve even distribution of nanoparticles in the polymer, which affects the final properties of the composites. Besides, oxidation and β-scission lead to degradation of polymer during melt mixing, not to mention that this method is energy intensive. In this study, solvent evaporation, wet phase inversion, and organic–inorganic hybridization were combined to design a novel asymmetric PU membrane with *in situ*-generated nano-TiO_2 (PUNT) as an ideal wound dressing. After a solvent evaporation process, organic–inorganic hybridization occurred synchronously as PU solution coagulated by wet phase inversion. The PUNT membrane according to this design consisted of an integral, dense skin layer supported by a porous sublayer, with well-separated nano-TiO_2 particles dispersed evenly throughout the sample. Because of this special structure, the crucial performances of the PUNT membrane fitted the basic requirements of an ideal wound dressing. Finally, the curative effect of the PUNT membrane was evaluated by *in vivo* animal study using rat model.

EXPERIMENTAL

Materials

The commercial biomedical PU resin (BioSpan, 20 wt % solution in *N*,*N*-dimethylacetamide) used in this study was supplied by Polymer Technology Group (United States). It was synthesized from methylene diphenylene diisocyanate, polytetramethylene oxide with molecular weight of 2000 g/mol, and mixed diamine chain extenders (ethylenediamine and 1,3-cyclohexanediamine). Tetrabutyl titanate and acetylacetone were purchased from Aldrich Chemical (United States). Anhydrous *n*-butanol and acetic acid were obtained from Junsei Chemical (Japan). Tegaderm (3M) brand commercial PU membrane dressing (9543HP) was used as a comparison material.

Membrane preparation

The modification of tetrabutyl titanate was performed under dry argon with Schlenk-line technique to avoid any partial hydrolysis by atmospheric moisture. A predetermined amount of tetrabutyl titanate (converted into TiO_2 concentration, by weight of the solid content in BioSpan) was added dropwise under stirring into an optimized volume of acetylacetone diluted with *n*-butanol (the molar ratio of acac : Ti was 4 : 1). This mixture was ultrasonicated for 1 h to obtain a transparent and yellow solution. The modified nanoprecursor prepared above was then dissolved in BioSpan under ultrasonic oscillation. After degassed adequately, the mixture was cast on a polytetrafluoroethylene release paper to a thickness of 150 μm using a Gardner knife. The casting solution was preheated at 50°C for 5 min with a dry argon stream for solvent evaporation before immersed into an aqueous bath at 25°C (pH 4.5–5.0, adjusted by acetic acid) for 30 min. During the wet phase inversion process, as the PU solution coagulated, the nanoprecursor hydrolyzed and condensated, *in situ* generating inorganic nano-TiO_2 particles in the organic PU membranes. Finally, the resultant membranes were rinsed in distilled water and dried at 50°C for 24 h. The membrane samples in this study were referred to as PUNT-*x*, wherein PU and NT represented polyurethane and nano-TiO_2, respectively, while *x* showed the TiO_2 concentration.

SEM/AFM analysis

Scanning electron microscope (SEM, Hitachi Model S520, Japan) was used to observe the cross-section morphologies of PUNT membranes. The cross sections were prepared by cryogenically fracturing the membranes in liquid nitrogen and then coated with aurum before observation. The morphologies of membrane surfaces were observed by atomic force microscope (AFM, SHIMADZU, SPM-9600, Japan) at ambient temperature using a tapping mode.

Measurement of WVTRs

WVTRs of the PUNT membranes were determined according to a published method.[10] A specially

designed cup containing human plasma was sealed with sample in such a manner that the cup mouth defined the area of the sample exposed to the environment. Human plasma (supplied by the Blood Bank at West China Hospital) was adopted because it was similar in composition to wound exudates. The edges of the sample were thoroughly sealed to prevent plasma leakage. Then, the assembly was hanged inverted in a test chamber at 35°C ± 0.5°C, with a constant relative humidity of 35% ± 1%. The selected temperature corresponded to the average surface temperature of injured skin reported by Lamke et al.,[11] and the relative humidity fell within the range of 22–49% observed by Wu for a hospital burns ward.[12] The weight change of permeation cup was recorded after 24 h, and the WVTR was calculated by the following equation.

$$\mathrm{WVTR} = \frac{a_1 - a_2}{S},$$

where $(a_1 - a_2)$ is the weight change of permeation cup (g) and S is the area of permeation (m^2).

Measurement of gas permeability

Gas (H_2, N_2, and O_2) permeation testing of PUNT membranes was conducted by using Yanaco GTR-10 gas permeability analyzer (Japan). The testing temperature was 35°C ± 0.5°C, and the pressure difference over the membranes was 1 atm. When the plot of Q (cm^3, the amount of gas that permeated through the sample) versus t (s, testing time) became linear, a steady-state gas permeability coefficient P (cm^3 cm/cm^2 s atm) could be calculated as follows.

$$P = \frac{dQ/dt}{S \times \Delta p/l},$$

where S and l stand for the permeation area (cm^2) and the sample thickness (cm), respectively; Δp is the pressure driving force (atm).

Nitrogen adsorption/desorption experiment

Low-temperature nitrogen adsorption/desorption experiments were conducted to determine the pore information and specific surface area of PUNT membranes at the boiling temperature of liquid nitrogen (−196°C) by using ASAP 2020 Accelerated Specific Surface Area and Porosimetry Analyzer from Micromeritics (United States). Samples were degassed overnight at 100°C under high vacuum before analysis. The obtained adsorption/desorption isotherms provided information on total pore volume (V_{tot}) and size distribution in micro-(pore diameter $d < 2$ nm), meso-($2 < d < 10$ nm), and macropore range. V_{tot} was obtained at the condition near to the saturation pressure $p/p_0 = 0.99$. The Horvath–Kawazoe (HK) model was used for micropore size calculation. In meso- and macrodomain, classical thermodynamic Barrett–Joyner–Halenda (BJH) theory was used. Brunauer–Emmitt–Teller (BET) theory was applied for specific surface area calculation from the obtained adsorption isotherms. The range of fit for the BET equation was restricted to nitrogen relative pressure (p/p_0) from 0.05 up to 0.35.

PBS solution absorption

The water absorption and equilibrium water content of PUNT membranes were determined by swelling the samples in pH 7.4 of phosphate-buffered saline (PBS) at 35°C ± 0.5°C. A known weight of PUNT membrane was placed in the PBS media for 7 days to reach equilibrium. Then, the sample was weighed immediately after it was blotted with filter paper to remove excessive surface water. The water absorption and equilibrium water content were calculated as follows.

$$\text{Water absorption } (\%) = \frac{W_s - W_0}{W_0} \times 100\%$$

$$\text{Equilibrium water content } (\%) = \frac{W_s - W_0}{W_s} \times 100\%,$$

where W_s is the weight of swollen sample and W_0 is the initial sample weight.

Bacteria experiments

Pseudomonas aeruginosa (*P. aeruginosa*, ATCC 27317, Gram-negative), *Escherichia coli* (*E. coli*, ATCC 25922, Gram-negative), and *Staphylococcus aureus* (*S. aureus*, ATCC 25923, Gram-positive) were selected as indicators of experimental bacteria, as they remain the most common and dangerous pathogen in burn injuries.[13,14] Bacteria were cultivated in Luria Bertani (LB) broth at 37°C for 24 h and diluted to 1×10^5 CFM/mL with sterile distilled water.

Bacteria penetration experiment was carried out using an assembly composed of an automatic injector and a filtration cell, which was drawn schematically in Figure 1. Samples with diameter of 5 cm were cut from the PUNT membranes. They were sterilized with ethylene oxide gas, sandwiched by two flat rubber gaskets to prevent fluid leakage, and mounted on the perforated stainless steel disk (diameter of 2.5 cm) in the filtration cell. Before injecting a suspension of *P. aeruginosa*, *E. coli*, or *S. aureus* (1×10^5CFM/mL) through the sample, preconditioning was conducted by injecting sterile distilled water for five times. The injection pressure was kept

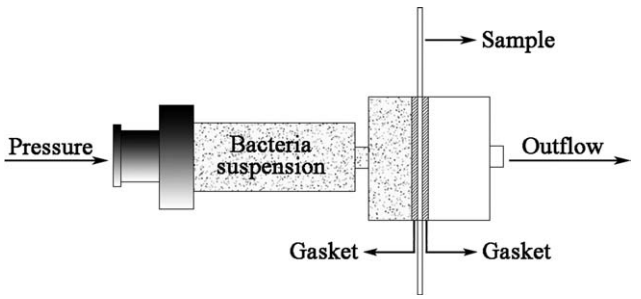

Figure 1 Schematic illustration of bacteria penetration experiment.

at 1 atm. The presence of bacteria in the outflow was checked by agar plate culture method.

The antibacterial activity of PUNT membranes was measured by shake flask testing according to the national standard GB15979-2002 defined by the Public Healthy Department of China: (1) Sample pieces (5 g) were sterilized with ethylene oxide gas before use and then put into a 250-mL flask with 5 mL bacteria suspension (1×10^5 CFM/mL) and 70 mL phosphate-buffered saline. (2) The mixed solution was shook on an agitation shaker with the speed of 300 rpm/min at 25°C for 2 h. This process was exposed to UVA (315–400 nm) irradiation from two 20 W black light lamps (Philips, Holland). The UVA intensity was determined to be 1 mW/cm^2 by a UVR-400 radiometer (S-365 UV-sensor, wavelength sensitivity of 315–400 nm, Iuchi, Osaka, Japan). The distance between the light source and the mixed solution was set at 20 cm. (3) The bacteria concentrations before and after shaking could be counted by agar plate counting method. The antibacterial activity was calculated as follows.

$$\text{Antibacterial activity } (\%) = \frac{A - B}{A} \times 100\%,$$

where *A* and *B* are the bacteria concentrations before and after shaking, respectively.

Cell adhesion and proliferation

Cell adhesion and proliferation on PUNT membranes were investigated to evaluate cytotoxicity according to ISO 10993-5. Test samples (1 cm in diameter) cut from PUNT membranes were washed with 99% ethanol for three times and then immersed in 70% aqueous ethanol for 24 h for sterilization. After washed with PBS three times to remove residual alcohol, the test samples were placed into the center of wells in a 24-well plate, respectively. Then, L929 fibroblasts (1×10^5 cells) in 2 mL Dulbecco's modified Eagle medium with 10% fetal calf serum were seeded onto the samples. Polystyrene well and latex were used as negative and positive control, respectively. After incubated at 37°C with 5% CO_2 for 3 days, the attached cells on samples were fixed with 0.5% glutaraldehyde, washed with PBS three times, and dehydrated in ethanol graded series. Finally, the samples were treated with *tert*-butanol for ethanol replacement and dried by CO_2 critical point drying method. The attached cells were aurum deposited in vacuum and observed by SEM.

The cell proliferation was measured after the cells were seeded for 1, 3, and 7 days, respectively, using the procedure of MTT (methyl thiazolyl tetrazolium) assay.

In vivo wound healing test

The curative effect of PUNT-4 was evaluated by using rat model. Male rats aged 3 months and weighing 300 ± 50 g were anesthetized with an intramuscular injection of pentobarbital at a dose of 50 mL/kg of body weight. Then, the dorsal hair of each animal was shaved. After the dehaired area was disinfected with 70% ethanol, a full thickness wound with a surface area of 2 cm × 2 cm was excised from the back of each rat. For comparison, the rats were divided randomly into three groups ($n = 25$/group). The wound surfaces in one group were dressed with an equal size of PUNT-4, and the other two groups were covered with sterile gauze and Tegaderm (9543HP), respectively. The treated animals were kept in separate cages and fed with commercial rat feed and water *ad libitum* during the healing period. The size of the wound was measured at 3rd, 6th, 12th, 15th, 18th, and 21st day, and the percentage of wound healing was calculated by the ratio of the observed size to the original wound size. The mean ± standard deviation of samples in each group was reported.

Statistics

The reported data were mean ± standard deviation of quintuplicate samples for each measurement. Statistical analysis was performed with Student's *t*-test. $P < 0.05$ was accepted as statistically significant.

RESULTS AND DISCUSSION

Membrane morphologies

By combining solvent evaporation, wet phase inversion, and organic–inorganic hybridization, a novel asymmetric PU membrane with *in situ*-generated nano-TiO_2 was prepared in this study, which fitted the basic requirements of an ideal wound dressing. During the solvent evaporation process, the loss of solvent drove the outermost region of the original polymer solution to form an integral and dense skin

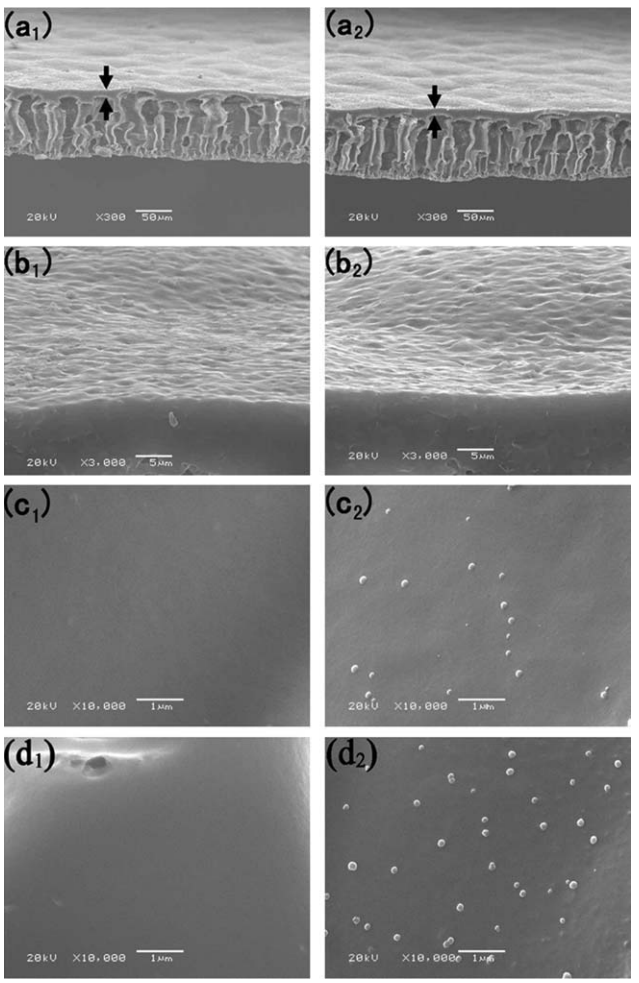

Figure 2 SEM images concerning the cross section of PUNT membranes. (a_1) whole image of PUNT-0; (a_2) whole image of PUNT-5; (b_1) skin layer of PUNT-0 (3000×); (b_2) skin layer of PUNT-5 (3000×); (c_1) skin layer of PUNT-0 (10,000×); (c_2) skin layer of PUNT-5 (10,000×); (d_1) sublayer of PUNT-0 (10,000×); and (d_2) sublayer of PUNT-5 (10,000×).

layer. This skin layer was expected to provide a barrier on wound beds against outside contamination. The underlying polymer solution with formed skin layer was then immersed into a coagulation bath, in which wet phase inversion was induced by diffusion of nonsolvent into and solvent out of the polymer solution. Because of this solvent/nonsolvent exchange, the underlying polymer solution separated into a polymer-rich and a polymer-lean phase. The former resulted in polymer skeleton, and the latter formed the pores. This porous sublayer was designed as a reservoir for excessive exudates on the wound beds. While the sublayer shaped during wet phase inversion, nanoprecursor hydrolyzed and condensated, *in situ* generating inorganic nano-TiO_2 throughout the organic PU membrane. Through this organic–inorganic hybridization, crucial performances of the PUNT membrane as a wound dressing were promoted, which were beneficial for rapid and proper wound healing.

Figure 2 illustrates SEM images concerning the cross-section morphologies of PUNT membranes. It was revealed that the PUNT membranes exhibited double-layer structure as designed. The outmost layer was integral and dense, $\sim$ 10 μm, and the sublayer exhibited a finger-like porous structure. Despite the *in situ* generation of nano-TiO_2, this asymmetric morphology did not change significantly. Higher magnification further showed that the *in situ*-generated TiO_2 particles were well separated and dispersed evenly in both skin layer and sublayer. The size of these particles ranged from 70 to 130 nm. As the sublayer surface would contact the wound beds directly, the morphologies of this surface were specially investigated by AFM, and the results are illustrated in Figure 3. Similar to those in the cross section, the *in situ*-generated TiO_2 particles on the sublayer surface were also in nanoscale and dispersed evenly. As already known, tetrabutyl titanate is an extremely moisture-sensitive compound. Its rapid hydrolysis and condensation in BioSpan that unavoidably contained a tiny amount of moisture yielded undesirable TiO_2 agglomerates and precipitates. Therefore, acetylacetone (acacH) was adopted in this study as a chelating agent to reduce the chemical reactivity of the nanoprecursor. According to prior report,[15] the chelating product was assumed to be $Ti(OC_4H_9)_{3-x}acac_x$ based on the following reaction.

$$Ti(OC_4H_9)_4 + x\text{acacH} \rightarrow Ti(OC_4H_9)_{3-x}acac_x + xC_4H_9(OH).$$

By substituting the easily hydrolyzable alkoxy groups, the less reactive Ti-acac groups acted as poisons toward hydrolysis and condensation, restraining the presence of TiO_2 agglomerates and precipitates in the PU membrane. On the other hand, the formation of TiO_2 could be hindered sterically by the PU macromolecular matrix, which also helped to keep their size in nanoscale and prevent agglomeration.

Water vapor transmission rate and gas permeability

Exudate retention below a wound dressing, caused by poor WVTR, or the dehydration of a granulating wound bed, caused by rapid water loss, can pose serious problems to the healings of wounds. An ideal wound dressing therefore should control evaporative water loss from a wound at an optimal rate, preventing excessive dehydration and exudate accumulation. Lamke et al. reported that the WVTRs for normal skin, first degree burns, and granulating

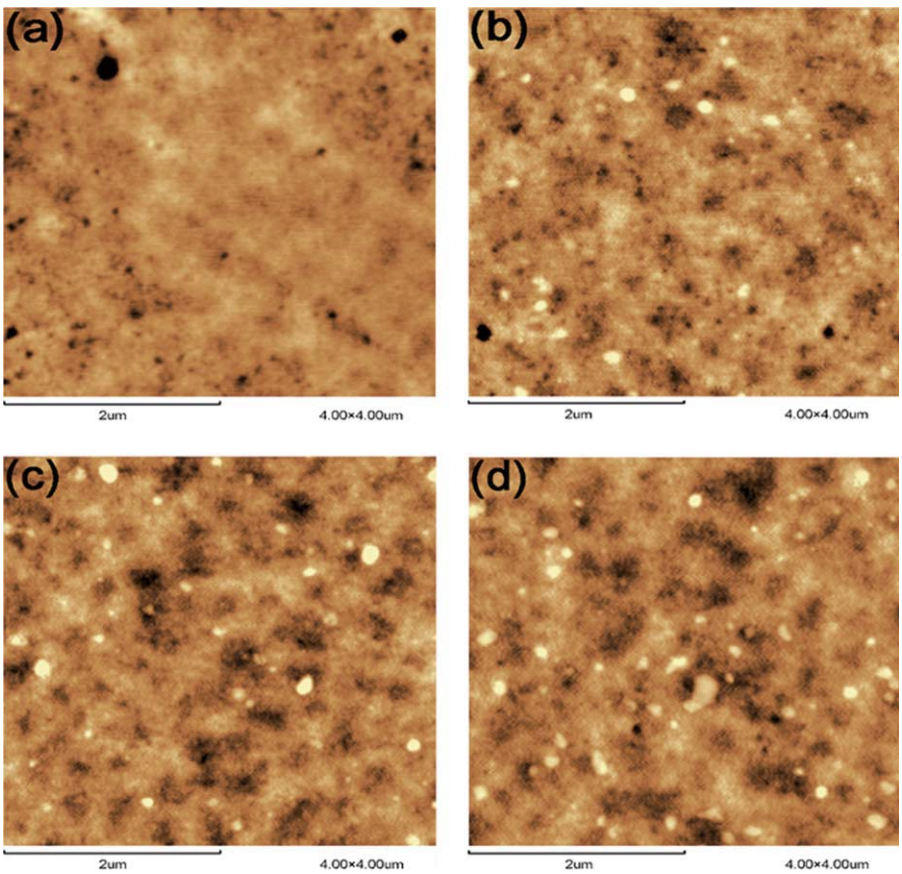

Figure 3 AFM images concerning the sublayer surface of PUNT membranes. (a) PUNT-0, (b) PUNT-1, (c) PUNT-3, and (d) PUNT-5. [Color figure can be viewed in the online issue, which is available at wileyonlinelibrary.com.]

wounds are 204 ± 12, 279 ± 26, and 5138 ± 202 g/m^2 day, respectively.[11] It was further recommended by Wong that wound dressings with WVTRs in the range of 2000–2500 g/m^2 day, half the loss of granulating wounds, would be sufficient to give adequate moisture and prevent exudate accumulation.[16] Typical PU membrane dressings commercially available include Tegaderm (3M), Bioclusive (Johnson-Johnson), and Op Site (Smith & Nephew), which have WVTRs of 491 ± 44, 394 ± 12, and 792 ± 32 g/m^2 day, respectively.[17,18] Such low WVTRs lead to the exudate accumulation, decelerating the healing process, and risking of bacteria contamination. In this study, special membrane-forming method and organic–inorganic hybridization were combined to prepare PU membrane dressing with ideal WVTR. Table I shows the WVTRs and gas (H_2, N_2, and O_2) permeability coefficients of various PUNT membranes. It could be seen that the WVTRs were as high as 1258–2689 g/m^2 day and increased with increasing nano-TiO_2 concentration. According to Wong's recommendation, it seemed that PUNT-3 and PUNT-4 were quite suitable as dressing membranes in terms of WVTRs. Similarly, the gas permeability coefficients also increased with increasing nano-TiO_2 concentration. Increased gas permeability could improve gas exchange through the dressing membranes, which was beneficial for oxygen-requiring reparative processes.

According to conventional principle, adding impermeable filler particles to polymer will lead to a systematic reduction in mass transport. Physically, such barrier phenomenon can be attributed to an increased diffusion path length, as penetrants are forced to take a tortuous course around filler particles to traverse a membrane.[19] However, the establishment of such principle is based on the assumption that the surface of the filler particles is completely wetted by surrounding polymer. It does not take account of the interfacial effects between polymer and some special fillers such as inorganic nanoparticles. As for the permeability behaviors of PUNT membranes in this study, the deviate from conventional prediction could be ascribed to the incompatibility between organic PU and inorganic nano-TiO_2, which resulted in pores at the interface. The effects of these interfacial pores became influential because of the tremendous surface area of nano-TiO_2. In the process of mass transportation, these pores helped mass diffusion and consequently resulted in an increase in permeability. SEM and AFM were useful for visualizing composite morphologies but did not readily reveal delicate

TABLE I
WVTRs, Gas Permeability Coefficients (P), and Total Pore Volume (V_{tot}) of PUNT Membranes

Sample	WVTR (g/m^2 day)	$P \times 10^{-7}$ (cm^3 cm/cm^2 s atm)			$V_{tot} \times 10^{-3}$ (cm^3/g)
		H_2	N_2	O_2	
PUNT-0	1258 ± 29	451 ± 7	26 ± 1	134 ± 4	4.41 ± 0.05
PUNT-1	1435 ± 34	538 ± 10	29 ± 1	156 ± 3	4.62 ± 0.07
PUNT-2	1871 ± 20	605 ± 8	32 ± 1	189 ± 3	4.77 ± 0.05
PUNT-3	2267 ± 31	686 ± 7	36 ± 2	208 ± 5	4.96 ± 0.05
PUNT-4	2412 ± 26	739 ± 8	39 ± 2	219 ± 3	5.12 ± 0.04
PUNT-5	2689 ± 37	819 ± 14	43 ± 1	233 ± 5	5.32 ± 0.06

interfacial structure between components. Therefore, nitrogen adsorption/desorption experiment was performed to confirm the existence of such interfacial pores.

Pore information and specific surface area of PUNT membranes

Nitrogen adsorption/desorption experiment provides a convenient way to characterize the pore information and specific surface area of porous materials. The total pore volumes of PUNT membranes are shown in Table I. The detected values increased as nano-TiO_2 concentration increased. This indicated that the *in situ* generation of nano-TiO_2 created extra pores in the PU membranes. To provide detailed information about these extra pores, the pore size distribution of PUNT membranes was calculated by using HK model for micropore, and BJH model for mesopore and macropore, respectively. By comparing the pore size distribution of different PUNT membrane throughout the entire size range, the only difference was found in the mesopore diameter range as displayed in Figure 4. It was revealed that all the other PUNT membranes contained extra mesopores compared with PUNT-0, and the size of these extra mesopores increased with increasing nano-TiO_2 concentration, varying from 2.6 nm for PUNT-1 to 3.3 nm for PUNT-5. These results indicated that the incompatibility-induced interfacial pores mentioned previously did exist in the PUNT membranes, and it seemed as if the more nano-TiO_2 *in situ* generated, the more significantly such incompatibility worked.

Another evidence for the presence of extra pores in PUNT membranes could be obtained from the analysis of specific surface area of samples. As illustrated in Figure 5, the BET specific surface area of PUNT membranes was plotted against the nano-TiO_2 concentration. If *in situ*-generated TiO_2 particles were completely wetted by PU, a linear decrease of specific surface with increasing TiO_2 concentration was expected (represented by the dashed line). As for the measured values, however, sharp deviate was recorded. The more nano-TiO_2 *in situ* generated, the higher BET specific surface the sample exhibited. This distinct deviation could also be ascribed to the formation of pores between organic–inorganic

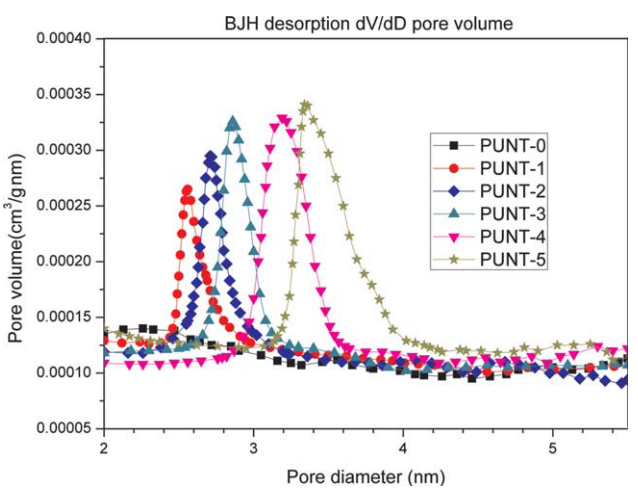

Figure 4 Mesopore size distribution of PUNT membranes. [Color figure can be viewed in the online issue, which is available at wileyonlinelibrary.com.]

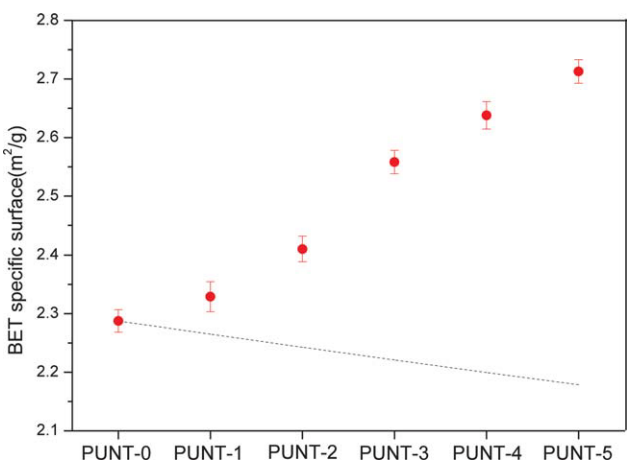

Figure 5 BET specific surface area of PUNT membranes. The dashed line represents the theoretical decrease that could be expected when the *in situ*-generated TiO_2 was completely wetted by surrounding PU. [Color figure can be viewed in the online issue, which is available at wileyonlinelibrary.com.]

TABLE II
Water Absorption and Equilibrium Water Content of PUNT Membranes

Sample	Water adsorption (%)	Equilibrium water content (%)
PUNT-0	489.5 ± 9.2	83.2 ± 0.2
PUNT-1	527.6 ± 4.5	84.1 ± 0.3
PUNT-2	559.0 ± 7.7	84.9 ± 0.3
PUNT-3	582.3 ± 6.4	85.5 ± 0.2
PUNT-4	610.9 ± 8.6	86.3 ± 0.2
PUNT-5	653.2 ± 5.9	86.9 ± 0.2

phases, which created extra specific surface for the PU membranes.

Fluid absorption capability

The capability to absorb excessive exudates from the wound beds is another important characteristic for an ideal dressing. In general, commercially available PU membrane dressings exhibit low fluid absorption capability due to their totally dense structure. For example, the water absorption of Tegaderm, Bioclusive, and Op Site is only in the range of 31–46%.[18] As a consequence, their applications are limited to low exudates cases, or exudates accumulation and infection occur. Table II shows the water absorption and equilibrium water content of various PUNT membranes. Because of the porous sublayer designed as a reservoir for exudates, the water absorption of PUNT membranes was in the range of 489.5–653.2%. These high values, according to previous literature,[18,20] were enough to prevent wound beds from exudate accumulation. On the other hand, the water absorption increased with increasing nano-TiO_2 concentration. This was because the extra interfacial pores between PU and nano-TiO_2 were beneficial for more capillary adsorbed water. In addition, the equilibrium water content of PUNT membranes was also much higher than those of Tegaderm, Bioclusive, and Op Site, which are as low as 21–36%.[18] High equilibrium water content guaranteed a moist environment over the wound beds.[18,20]

Bacteria penetration and *in vitro* antibacterial activity

To protect the wound beds from outside microorganism, an ideal dressing should act as a barrier against microorganism penetration. In this study, no bacteria were detected in the outflow through PUNT membranes, despite that the pore size at the sublayer of the PUNT membranes was much larger than the minimal size of the bacteria (0.5 μm). This impermeability should be attributed to the integral and dense skin layer of samples formed in the solvent evaporation process.

Although the PUNT membranes could exclude outside bacteria, bacteria survived in the depth of sweat glands and hair follicles might still colonize the wounds easily to cause infection after injury, unless topical antibacterial agents were used.[21] Table III shows the antibacterial activity of PUNT membranes measured by shake flask testing. It was found that PUNT-0 exhibited almost no antibacterial activity against *P. aeruginosa*, *E. coli*, or *S. aureus*, whereas the antibacterial activity of other PUNT membranes increased with increasing nano-TiO_2 concentration. Especially for PUNT-4 and PUNT-5, the percentage reduction ratios for three stains exceeded 68%. The origin of such antibacterial activity could be ascribed to the well-known photocatalytic activity of TiO_2. In brief, when exposed to ultraviolet light ($\lambda < 400$ nm), TiO_2 will be activated to generate electron-hole pairs. The electrons reduce oxygen to produce superoxide anions. The holes oxidize water to produce hydroxyl radicals. These reactive species are powerful for degrading organic pollutants, such as bacteria and viruses.[22,23]

The chemistry of tetrabutyl titanate to produce TiO_2 has been established for decades. As the PUNT membranes were prepared without calcination, the *in situ*-generated nano-TiO_2 should be mostly present in an amorphous form with hydrated water molecules ($TiO_2.nH_2O$).[24–26] Previous literature claimed that amorphous TiO_2 was inactive compared with crystallite forms because it contained high concentrations of defects that functioned as rapid electro-hole recombination centers.[27] However, the amorphous TiO_2 used in this literature was nonhydrated, because it was precalcined at around 300–400°C before use. Actually, the presence of hydrated water could substantially suppress the recombination of holes with electrons at defects, making amorphous $TiO_2.nH_2O$ active, or antibacterial herein, as TiO_2 crystallites.[26] Additionally, the extremely high surface area of nanoscaled TiO_2 facilitated the adsorption of target bacteria, which accelerated the rate of antibacterial reaction.[28] Therefore, although containing amorphous TiO_2, the PUNT membranes still exhibited obvious antibacterial activity. In fact, the photocatalysis of hydrated form of amorphous TiO_2 had been reported in many literatures.[25,26,29]

TABLE III
Antibacterial Activity of PUNT Membranes

Sample	Antibacterial activity (%)		
	P. aeruginosa	*E. coli*	*S. aureus*
PUNT-0	2.6 ± 0.6	3.2 ± 0.9	2.2 ± 1.1
PUNT-1	32.3 ± 2.1	22.0 ± 1.8	28.1 ± 2.5
PUNT-2	47.2 ± 1.9	35.4 ± 2.2	40.5 ± 2.4
PUNT-3	58.3 ± 2.7	49.3 ± 2.0	54.8 ± 1.9
PUNT-4	74.0 ± 1.9	68.6 ± 2.8	70.3 ± 2.6
PUNT-5	86.9 ± 2.3	78.5 ± 1.7	81.5 ± 2.2

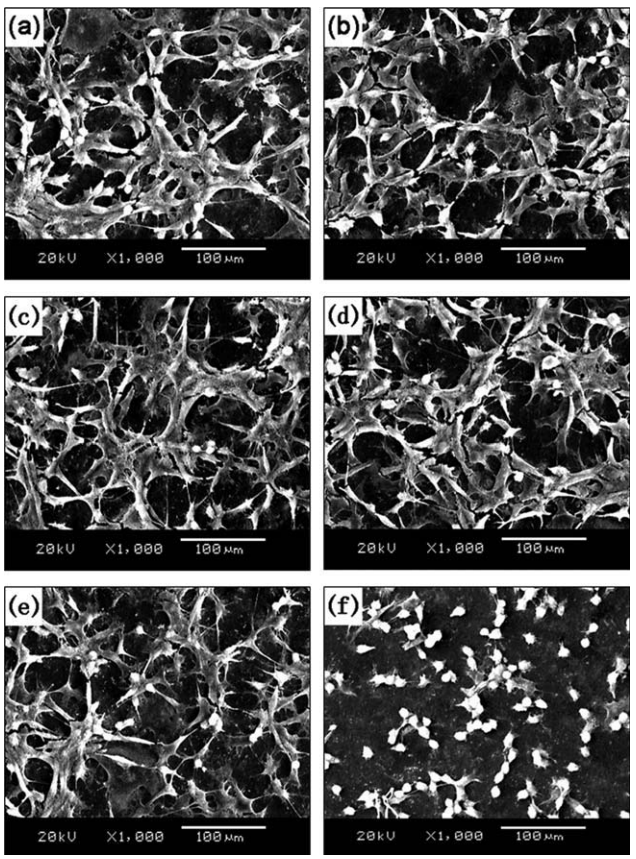

Figure 6 Morphologies of L929 fibroblasts on PUNT membranes, polystyrene well (negative control), and latex (positive control) after incubating for 3 days. (a) PUNT-0, (b) PUNT-1, (c) PUNT-3, (d) PUNT-5, (e) polystyrene well, and (f) latex.

Cytotoxicity

As specified by the supplier, BioSpan shows no cytotoxicity. However, after any modification such as incorporating aggressive antimicrobial agents, cytotoxic effect may be induced. The morphologies of L929 fibroblasts adhesive on PUNT membranes, polystyrene well (negative control), and latex (positive control) after 3 days of seeding are shown in Figure 6. The cells on PUNT membranes showed similar morphologies to those on polystyrene well. They all exhibited typical fibroblast morphologies, an elongated and polygonal shape. However, few cells on latex elongated as they were influenced by toxic materials released from latex. Figure 7 shows the MTT absorbance in cell proliferation experiment. No significant difference among PUNT membranes was found after the same testing time. They were all significantly better at promoting cell proliferation than negative control. The MTT absorbance of latex positive control was significantly lower than negative control throughout the testing period. This was because the cells were damaged and finally died by toxic materials released from latex. According to these results and the evaluation criteria defined in ISO 10993-5, it could be concluded that the *in situ*-generated nano-TiO_2 in PUNT membranes wound not induce any cytotoxicity to the seeded cells.

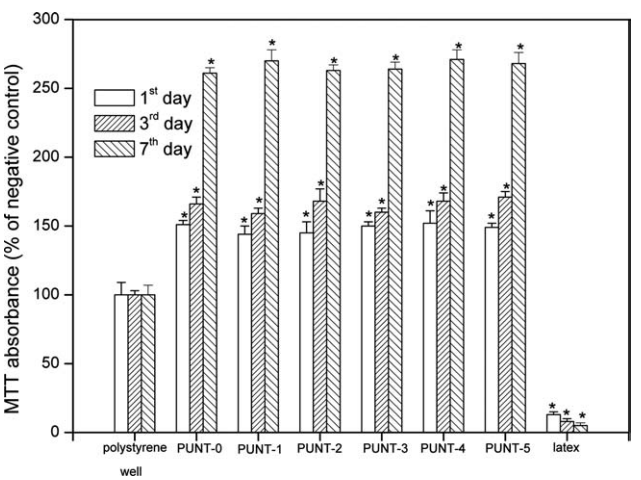

Figure 7 Cell proliferation on PUNT membranes, polystyrene well (negative control), and latex (positive control). The absorbance was normalized with that of negative control at each time interval. *$p < 0.05$ compared with negative control.

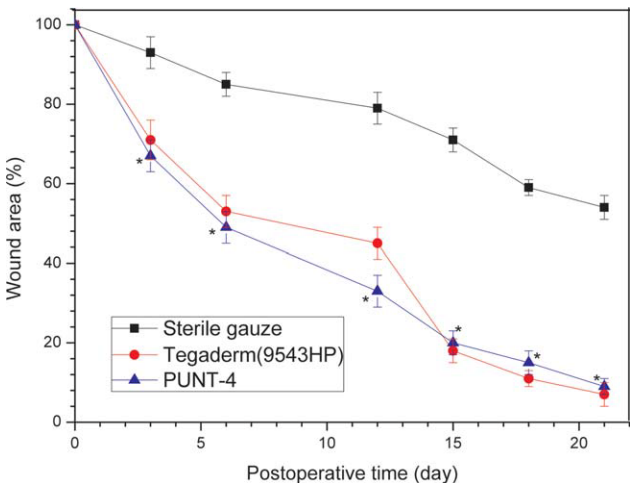

Figure 8 Comparison of gauze, Tegaderm (9543HP), and PUNT-4 in animal test. *$p < 0.05$ compared with gauze. [Color figure can be viewed in the online issue, which is available at wileyonlinelibrary.com.]

In vivo wound healing test

After comprehensive consideration, PUNT-4 was chosen in the animal test to compare its curative effect with some other dressings. Figure 8 illustrates the reduction in wound areas at different postoperative time using PUNT-4, sterile gauze, and Tegaderm (9543HP), respectively. The wound area decreased gradually and reached 54% after 21 days for sterile gauze. In the case of Tegaderm (9543HP)-treated wound beds, the healing rate was faster and

about 93% wound closure was achieved at the end of the test. As for wounds covered with PUNT-4, the percentage of wound healing almost equivalent to those treated with Tegaderm (9543HP) was observed after the same interval time. Except for the above statistical data, some other important facts observed during the animal test were worth noting. After only 6 days in the test, dried scabs began to appear on wound beds dressed with gauzes. The fibers of the gauzes become trapped in the nascent tissue, which made uncover of gauzes for measuring the wound area difficult. This was because gauzes exhibited excessive WVTR, and thus they could not maintain a moist environment at the wound/dressing interface. Obvious exudate leakage could be observed on wounds dressed with Tegaderm (9543HP). At the 9th day in the test, infections were encountered on six Tegaderm (9543HP)-treated rats, four of whom even sacrificed at the 15th–17th day. We thought that this phenomenon was due to the poor WVTR and fluid absorption capability of Tegaderm (9543HP), which hindered the removal of exudates that contained nutrients for the bacteria. Favorably, PUNT-4 was found to adhere uniformly on the wound surface without any exudate leakage observed. It could also be peeled off smoothly from the wound beds. The healed area was healthy clean, pinkish red in color, and glistening in appearance. Considering the above facts and the statistical data present in Figure 8, it suggested that the curative effect of PUNT-4 was better than gauze and Tegaderm (9543HP).

CONCLUSIONS

By combining solvent evaporation, wet phase inversion, and organic–inorganic hybridization, a novel asymmetric PU membrane with *in situ*-generated nano-TiO_2 (PUNT) was successfully prepared for application as an ideal wound dressing. An integral and dense skin layer was formed during the solvent evaporation process, and the following wet phase inversion and synchronously occurred organic–inorganic hybridization could produce a porous sublayer and evenly distributed nano-TiO_2 throughout the sample. Each component part of this PUNT membrane could serve respective function on wound beds to provide a suitable environment for proper healing. The skin layer prevented bacteria penetration, and the sublayer could absorb high amounts of exudates. In the presence of *in situ*-generated nano-TiO_2, this PUNT membrane could control evaporative water loss from wound beds at an optimal level and absorb more exudates, keeping the wound beds moist without risking dehydration or exudates accumulation. Nano-TiO_2 also promoted the gas permeability of PUNT membrane, which was beneficial to gas exchange between the wound and the environment. After nanomodification, the PUNT membrane became antibacterial against *P. aeruginosa*, *E coli*, and *S. aureus*, whereas still remained noncytotoxic. Animal studies suggested that the curative effect of this PUNT membrane was better than gauze and a commercial PU membrane dressing.

References

1. Livshits, V. S. Pharm Chem J 1988, 22, 515.
2. Ovington, L. G. Clin Dermatol 2007, 25, 33.
3. Yang, J. M.; Yang, S. J.; Lin, H. T.; Chen, J. K. J Biomed Mater Res B Appl Biomater 2007, 80, 43.
4. Hinrichs, W. L. J.; Lommen, E. J. C. M. P.; Wildevuur, Ch. R. H.; Feijen, J. J Appl Biomater 2004, 3, 287.
5. Kurdi, J.; Tremblay, A. Y. J Appl Polym Sci 1999, 73, 1471.
6. Ismail, A. F.; Lai, P. Y. Sep Purif Technol 2004, 40, 191.
7. Li, X.; Chen, C. X.; Li, J. D. J Membr Sci 2008, 314, 206.
8. Lee, W. J.; Kim, D. S.; Kim, J. H. Korean J Chem Eng 2000, 17, 143.
9. Jain, S.; Goossens, H.; Picchioni, F.; Magusin, P.; Mezari, B.; Duin, M. V. Polymer 2005, 46, 6666.
10. Queen, D.; Gaylor, J. D. S.; Evans, J. H.; Courtney, J. M. Biomaterials 1987, 8, 367.
11. Lamke, L. O.; Nilsson, G. E.; Reithner, H. L. Burns 1977, 3, 159.
12. Wu, P. PhD Thesis, Bioengineering Unit, Strathclyde University, Glasgow, 1993.
13. Agnihotri, N.; Gupta, V.; Joshi, R. M. Burns 2004, 30, 241.
14. Fang, S. D.; Xia, Z. P. Clinical Infection in Surgery; Shenyang Press: Shenyang, 1999.
15. Puri, D. M.; Pande, K. C.; Mehrotra, R. C. J Less-Common Met 1962, 4, 393.
16. Wong, P. MSc Thesis, University of Strathclyde, 1980.
17. Wu, P.; Fisher, A. C.; Foo, P. P.; Queen, D.; Gaylor, J. D. S. Biomaterials 1995, 16, 171.
18. Yoo, H. J.; Kim, H. D. J Appl Polym Sci 2008, 107, 331.
19. Merkel, T. C.; Freeman, B. D.; Spontak, R. J.; He, Z.; Pinnau, I.; Meakin, P.; Hill, A. J. Science 2002, 296, 519.
20. Yoo, H. J.; Kim, H. D. J Biomed Mater Res B Appl Biomater 2008, 85, 326.
21. Vindenes, H.; Bjerknes, R. Burns 1995, 21, 575.
22. Robertson, J. M. C.; Robertson, P. K. J.; Lawton, L. A. J Photochem Photobiol Chem 2005, 175, 51.
23. Acosta, D. R.; Martinez, A. I.; Lopez, A. A.; Magana, C. R. J Mol Catal A: Chem 2005, 228, 183.
24. Khalil, K. M. S.; Zaki, M. I. Powder Technol 1997, 92, 233.
25. Randorn, C.; Wongnawa, S.; Boonsin, P. Sci Asia 2004, 30, 149.
26. Zhang, Z.; Maggard, P. A. J Photochem Photobiol Chem 2007, 186, 8.
27. Ohtani, B.; Ogawa, Y.; Nishimoto, S. J Phys Chem B 1997, 101, 3746.
28. Kanna, M.; Wongnawa, S. Mater Chem Phys 2008, 110, 166.
29. Ruan, J. F.; Li, C. X.; Wang, Z. H. J Beijing Univ Chem Technol 2008, 29, 1.